d → d Spectrum and High-Spin/Low-Spin Competition in d^6 Octahedral Coordination Compounds: ab Initio Study of Potential Energy Curves

Hélène Bolvin†

Laboratoire de Physique Quantique, Université Paul Sabatier, 118 rte de Narbonne, 31062 Toulouse Cedex, France

Received: June 24, 1998; In Final Form: June 29, 1998

Ab initio calculations were performed, using the CASPT2 method and moderate-size basis sets, on several d^6 octahedral coordination compounds, $Fe(CN)_6^{4-}$, $Fe(NCH)_6^{2+}$, *cis*- and *trans*-$Fe(CN)_2(NCH)_4$, and $Cr(CO)_6$. The study concentrates on the six lowest states of the d → d spectrum (three singlets, one quintet, and two triplets states), and on the dependence of their energy on the metal−ligand equilibrium distance. It has been exended to a d^5 compound, $Fe(CN)_6^{3-}$. The spin multiplicity of the ground states is correctly reproduced, and the metal−ligand distances and the vertical transitions energies, and dissociation energies are in good agreement with experiment. From the potential energy curves, it is possible to extract Racah's parameters, *B* and *C*, and the crystal field parameter Δ as a function of the metal−ligand distance. The dependence of Δ on this distance is rationalized in terms of ligand field theory. Finally, the role of the triplet states in the spin transition is discussed.

1. Introduction

When the low-spin (LS) and the high-spin (HS) states of a coordination compound are nearly degenerate, it is possible to switch the molecule from one state to the other one by means of a change of temperature, of pressure, or by absorption of light: this phenomenon is called spin transition.[1−4] The family of quasi-octahedral compounds of Fe(II) presents most of the presently known spin transitions. In an octahedral environment, d orbitals of the metal ion are split into two groups, t_{2g} and e_g, by an energy Δ. When ligands are of strong field type, Δ is large and the t_{2g} orbitals are populated first to a double occupancy; the molecule is in a LS state. When Δ is small, electrons are spread over the whole set of d orbitals and the ground state is a HS state. For a d^6 compound, the LS state, in the $(t_{2g})^6$ configuration, is a singlet and the HS state, in the $(t_{2g})^4(e_g)^2$ configuration, is a quintet.

The key parameter determining the spin transition is the difference of energy between these two states, $E_{HL} = E_{HS} - E_{LS}$; it must be slightly positive for the phenomenon to take place. These two states do not have the same equilibrium geometry because of the antibonding character of e_g orbitals, which makes the metal−ligand distance larger in the HS state. Usually, competition between LS and HS state is described as the competition between the pairing energy of the electrons in d orbitals and Δ. In the LS state, the six electrons are paired, which costs 3*P*, *P* being the excess of repulsion energy of two electrons in the same orbital compared to their repulsion when they occupy two different d orbitals. In the HS state, only two d electrons are paired, and the energy of this state is roughly $P + 2\Delta$. When Δ is greater (smaller) than *P*, the LS (HS) state is favored. While *P* does not vary a lot with metal−ligand distance, Δ is very sensitive to it, and the above rule should be formulated taking into account the different geometries of the two states.

Calculation of E_{HL} requires the calculation of energies as a function of metal−ligand distance. Such calculations are more difficult than those of vertical transition energies because they necessitate an accurate evaluation of the reference energy at each geometry, or at least a distance-independent error. For such large systems, complicated by the influence of the crystal environment, presently available ab initio techniques can only afford a semiquantitative estimate of the relative position of the potential energy surfaces.

A d^6 spin transition requires the presence of an intermediate triplet state provided by the excited configuration $(t_{2g})^5e_g$ which couples with both the singlet and the quintet states through spin−orbit coupling. If it lies below the crossing point between LS and HS states, it will be an intermediate state in the dynamics of spin transition; if not, its energy will determine the magnitude of the coupling between LS and HS states via second-order spin−orbit coupling. Thermodynamical treatment of spin transition completely neglects these triplet states. The system is modelized by the mean of an Ising Hamiltonian,[5−8] each molecule being represented by a two-level system, the LS and the HS one, and the difference of energy between them, E_{HL}. Further molecular features are neglected. The interaction between two molecules is characterized by a parameter *J*; this enables to take into account cooperative effects necessary to describe phase transitions. The present calculations should indicate whether or not this model should be expanded to a three-state model (or more), including the triplet states.

One of the interesting features concerning the spin-transition compounds is the LIESST (light-induced excited spin-state trapping) effect. Starting from the LS state at very low temperature, the system is excited to the singlet state $^1T_1$ by absorption of light. Nonradiative pathways of desexcitation bring the system in the metastable HS state.[9−11] Knowledge of the excited states could help the understanding of such experiments, which combine vertical transition with diabatic de-excitations. Furthermore, the tunneling rate of de-excitation of the metastable state is governed by the distance between the

† E-mail: bolvin@irsamc1.ups-tlse.fr.

S1089-5639(98)02759-5 CCC: $15.00
Published on Web 08/28/1998

minima of the LS and HS states. It is then crucial to determine the decisive parameters of this phenomenon.

Calculations have been carried out on several molecular systems: (i) the two octahedral complexes of Fe(II), $Fe(CN)_6^{4-}$ and $Fe(NCH)_6^{2+}$, representing a LS and a HS complex, respectively; (ii) $Cr(CO)_6$ a strongly LS complex characterized by an important π back-donation; (iii) a d^5 compound, $Fe(CN)_6^{3-}$.

Crystallographic data and UV−visible spectra are available for all four species. Crystallographic data of some spin-transition compounds are known for both LS and HS states.[12] They show that the main difference between the two states is the distance between iron and ligands, this difference being on the order of 0.2 Å. The internal distances of the ligands are mostly unchanged. When the ligand is a chelate one, the ligand−iron−ligand angle is perturbed, and in most cases, the HS phase display the largest deviation from a strict O_h geometry. These data show that the dominant parameter is the metal−ligand distance. In the four complexes, potential energy curves have been calculated as a function of the size of the coordination sphere,while the internal geometry of the ligands was kept fixed and O_h symmetry was maintained.

Systems exhibiting spin-transition behavior are too large to have their excited states modelized by ab initio methods with some accuracy. To approach as close as possible a spin-transition complex, we have considered a mixed compound, $Fe(NCH)_4(CN)_2$, which represents an intermediate system between a LS and a HS molecule. This hypothetical system was treated with the same procedure as the previous ones in order to compare the results.

Two methods are applied here. First, the CASSCF/CASPT2 approach has recently been used with success in studies of the excited states.[13] It gives satisfying results for tetrahedral complexes of nickel(II), and recently, for biological systems like plastocyanin.[15] Pierloot et al. were able to reproduce the vertical spectrum of two of the complexes we deal with, $Fe(CN)_6^{4-}$ and $Fe(CN)_6^{3-}$ and from some other octahedral complexes.[16]

Second, DFT calculations give satisfying results for the calculation of excited states of quite large systems. Because the method is restricted to the lowest state in each symmetry, only the LS, the HS, and one triplet state have been calculated with this method.

The outline of this paper is as follows:

1. In section 2, we have determined the complete d → d spectrum of the Fe(II) atom in the same basis set later used on molecular calculations to check the ability of both the basis set and of the computational method to describe this spectrum.

2. Section 3 reports the various calculations performed on two of the complexes $Fe(CN)_6^{4-}$ and $Fe(NCH)_6^{2+}$ to calibrate the method. With the CASSCF/CASPT2 procedure, the effect of the basis set on the ligands, of the choice of active space, and of the point charges representing counterions have been checked. This procedure has furthermore been compared to DFT results.

3. With the chosen procedure, we have performed LS, HS, and the whole set of states derived from the monoexcited configurations for the six molecules $Fe(CN)_6^{4-}$, $Fe(NCH)_6^{2+}$, $Fe(NCH)_4(CN)_2$ in the cis and trans conformations, $Cr(CO))_6$, and $Fe(CN)_6^{3-}$ and compared with the available experimental data. These results are reported in section 4.

4. As shown in section 5, the resulting distance-dependent spectrum allows possible the extraction of the crystal field parameter Δ and of Racah's parameters B and C in terms of this distance. Δ will be well described by an exponential law compatible with the ligand field theory.

Some features of the effective interaction between LS and HS states, a crucial parameter in spin-transition phenomenon, are discussed in the Conclusion.

Reading of methodological sections 2 and 3 is not compulsory for the understanding of the physical results of sections 4 and 5.

2. Spectroscopy of Iron(II)

2.1. Methods and Details of the Calculations. In this section, we consider the d → d spectrum of iron(II). The aim of this study was not to reproduce experimental spectrum with the highest possible accuracy but to check whether the basis used in the molecular calculations is reasonable. The quality of the iron basis set is essential for the spectra of the complexes, since all the molecular excitations we are concerned with will be mostly localized on the metal center. Furthermore, the basis set of the bare ion is sufficiently small to allow a comparison of perturbative methods (CASPT2) with variational ones (CASDI).

The basis set used is of the generally contracted ANO (atomic natural orbital) type. The starting primitive set (17s12p9d4f) is contracted to [5s4p3d2f].[17] Two types of calculations were performed: a perturbative procedure using the MOLCAS quantum chemistry software[18,19] and a variational one using the recently written CASDI program.[20] All calculations were carried out in D_{2h} symmetry.

The first computational scheme consists of two major steps; first, in the CASSCF step, a multiconfigurational wave function is constructed for a given state, comprising all configurations obtained by distributing a given number of electrons (called the active electrons) in a given number of orbitals (the active orbitals). Configurational and orbital variational parameters are optimized in a single step. The active space has to include at least all orbitals that are crucial for the description of the states involved, namely the orbitals that will be partly occupied. We have employed two different active spaces in our study. The CAS1 consists of the five d orbitals, whereas in the CAS2 we have added five more d orbitals, both of them having six electrons. The significance of a second d shell in the active space has been discussed in earlier applications to transition-metal spectroscopy;[13] it ensures a better description of the correlation of the d electrons and of the spatial relaxation under changes of the orbital occupancies. This optimization can be done for each state separately or for an average over all the states of one symmetry of space and of spin. The second step is the calculation of the contribution to the correlation energy of the other electrons by mean of a second-order perturbation theory, CASPT2.

The second type of calculation is of variational type. Starting with a set of molecular orbitals, one considers the active space and an additional space (see below) comprising all or some single and double excitations out of it. In terms of the RAS formalism,[21] DDCIm (difference dedicated configuration interaction) spans the following space; with n_h (n_p) the number of allowed holes (particules) in RAS1 (RAS3), $n_h + n_p \leq m$.[22] Then the Hamiltonian matrix is written in this space and the first roots are calculated. It can be shown that at second order level of perturbation theory the determinants of the DDCI3 space are the only ones contributing to the energy difference between two states mainly described by eigenvectors of the CASCI. This space is further limited to the DDCI2 space when the two states in question differ only in their spin state and not by their orbital

TABLE 1: Spectroscopy of Iron(II) (All Values in cm^{-1})

		CASSCF		CASPT2		DDCI2	DDCI3	CASSD
	exp	CAS1	CAS2	CAS1	CAS2	CAS1	CAS1	CAS1
^3P	19 610	24 518−25 617	24733	18 905−20 056	19 419	20 709	20 365	20 543
^3H	19 829	22 665−23 277	22332	20 451−21 293	21 025	21 726	21 708	21 677
^3F	21 212	25 986−26 593	25538	21 315−21 627	22 138	22 857	22 626	22 723
^3G	24 414	28 565−29 113	28070	25 049−25 323	25 788	26 436	26 340	26 346
^1I	29 933	33 643−34 347	33193	31 444−35 435	32 178	32 105	32 571	32 639
^3D	30 361	36 902−37 517	36033	31 367−31 481	32 037	32 811	32 702	32 675
^1G	30 463	35 638−36 262	34963	31 449−31 892	32 333	32 911	32 678	32 700
^1S	34 389	41 503−41 955	40533	34 888−35 408	35 886			
^1D	35 381	44 085−44 937	43597	36 665−37 039	37 450	37 530	37 225	37 341
^1F	42 474	51 592−52 118	50405	43 963−44 474	44 927	45 788	45 579	45 615
^3P	49 570	60 215−61 387	58475	53 231−53 696	53 198	53 165	52 665	52 983
^3F	50 261	60 963−62 118	58844	51 750−52 373	52 446	53 631	53 071	53 449
^1G	57 222	68 775−69 266	66470	59 881−60 681	60 510			

part. In DDCI4, all the single and doubles are taken into account; it is namely a CASSD space. The variational calculations have been performed for CAS1 in the set of orbitals coming out from the state average CASSCF calculation relative to the triplet states.

2.2. Results. Results are given in Table 1. Almost the complete d → d spectrum has been calculated. For CAS1, the two given values are the two extreme ones, depending on the way orbitals were obtained, namely averaged for all the states of the symmetry or state-specific and depending on the symmetry (when reduced from the O_3 group to D_{2h}, terms may have components in different representations). Results do not depend too much on this choice, and for CAS2, energies are calculated with the averaged orbitals.

The inclusion of a second d shell in the CAS hardly influences the first roots, at both the CASSCF and CASPT2 levels. For the higher roots, the CASSCF excitations energies are improved, but at the CASPT2 level, the effect is small.

The size of the DDCI2, DDCI3, and CASSD spaces are 26 078, 195 006, and 657 790 determinants respectively. The close agreement between DDCI2 and DDCI3 results is quite surprising.

The CASSD results may be supposed to be close to the full CI limit. The CASPT2 results are quite close to the variational ones, the discrepancy being lower than 1000 cm^{-1} for all roots. The discrepancy between CASPT2 and experiment can certainly be ascribed to basis set limitations rather than lack of higher-order effects.

The experimental values given in this table are extracted from Moore tables[23] and *J*-averaged. Trees has shown that spin−orbit coupling introduces terms shifts never larger than 100 cm^{-1} [24] which is much less than the deviation of our results from experiment.

All the CASSD results above are the experimental ones. The discrepancy becomes greater for the higher roots; although it is less than 2000 cm^{-1} for the first ten, it is on the order of 3000 cm^{-1} for the final ones.

In conclusion, even if the basis set used is quite small, it is able to reproduce the main features of the d → d spectrum of iron(II). The discrepancy is greater for the highly excited states as the basis set has been optimized to describe the lowest states. One may notice that in highly excited states, the electrons generally are closer (lack of Fermi hole for low-spin states, increasing double occupation of d orbitals) and a correct treatment of their correlation would require larger basis sets with high-*l* orbitals. This remark should remain valid for the complexes; i.e., the HS error should be somewhat smaller than for the LS one. The main conclusions are (i) the multiconfigurational perturbative method gives results comparable to a quite large CI variational method; and (ii) the accuracy obtained with the chosen basis set is adequate for the following molecular calculations.

3. Assessment of the Methodology

$Fe(CN)_6^{4-}$ and $Fe(NCH)_6^{2+}$ have been used as benchmark molecules to establish a methodology able to describe such complexes with reasonable accuracy at a moderate price. Most of the results are given for $Fe(CN)_6^{4-}$; only the effect of point charges and the comparison between CASPT2 and DFT concern $Fe(NCH)_6^{2+}$.

3.1. Methods and Details of the Calculations. 3.1.1. CASSCF/CASPT2. These calculations have been performed with the MOLCAS 3 package, with the scheme CASSCF/CASPT2. The same basis as in section 2 has been used for the iron atom, namely an ANO basis with (17s12p9d4f) contracted to [5s4p3d2f]. For the ligands, many basis sets have been applied in order to check which was the smallest one giving satisfactory results. All basis sets are of ANO type: a single zeta set with (10s6p) contracted to [2s1p] (SZ); a double zeta set with (10s6p) contracted to [3s2p] (DZ); and a double zeta with polarization set that is the previous one augmented with a primitive d of exponent 0.344 for C atom and of exponent 0.5054 for N atom (DZP).

In all calculations, the internal geometry of the ligand is kept fixed with a bond length of 1.17 Å. The iron−metal distance is varied, maintaining the O_h symmetry. All calculations are formally performed in D_{2h} symmetry.

As in the previous section, we have used different choices of active spaces for the calculations. As before, CAS1 and CAS2 are (2111)/6 electrons and (4222)/6 electrons, respectively, in terms of irreps A_{1g}, B_{1g}, B_{2g}, and B_{3g}.

Pierloot[16] has suggested an alternative choice of the CAS to better describe the covalency of the complex: the σ nonbonding orbitals of the ligands which are more involved in the formation of the bond with the metal, and more precisely their combination of E_g symmetry, are added to the active space. CAS3 is (4222)/10 electrons; the second set of t_{2g} CASSCF orbitals does not converge on the three antibonding π orbitals of the ligands, as suggested by Pierloot, but remain the correlation d orbitals.

In the former CAS, $d_{t_{2g}}$ orbitals are better described than the d_{e_g} ones because they have two sets of orbitals. We performed a further calculation including two more virtual E_g orbitals to enable the d_{e_g} orbitals to relax and to be better correlated. Thus, CAS4 is (6222)/10 electrons.

$Fe(CN)_6^{4-}$ is highly negatively charged. Without any point charges balancing the large negative charge of the molecular edifice, many of the orbital energies are found to be positive at

TABLE 2: Metal−Ligand Distances and Transition Energies for $^1A_{1g}$ (LS), $^3T_{1g}$ (TS), and $^5T_{2g}$ (HS) States of $Fe(CN)_6^{4-}$

method	basis set	CAS[a]	R_{LS}, Å	R_{TS}, Å	R_{HS}, Å	ΔE_{TL}, eV	ΔE_{HL}, eV
CASSCF	DZ	CAS3	2.07	2.28	2.38	1.01	−0.35
CASPT2	SZ	CAS1	1.99		2.25		−0.05
CASPT2	DZ	CAS1	1.82	2.10	2.26	1.96	0.70
CASPT2	DZP	CAS1	1.81	2.10	2.30	2.02	0.72
CASPT2	DZ	CAS2	1.86	2.12	2.27	1.81	0.56
CASPT2	DZ	CAS3	1.90	2.06	2.26	2.17	1.37
CASPT2	DZ	CAS4	1.90	2.06	2.26	2.54	1.68
DFT	DZ		1.95	2.17	2.26	1.73	1.06

[a] CAS1 = 6el/5MO; CAS2 = 6el/10MO; CAS3 = 10el/10MO; CAS4 = 10el/12MO.

TABLE 3: Metal−Ligand Distances and Energy Gaps for $^1A_{1g}$ (LS), $^3T_{1g}$ (TS), and $^5T_{2g}$ (HS) States of $Fe(NCH)_6^{2+}$

method	basis set	CAS	point charges	R_{LS}, Å	R_{TS}, Å	R_{HS}, Å	ΔE_{TL}, eV	ΔE_{HL}, eV
CASPT2	DZ	CAS2	yes	1.90	2.05	2.10	0.39	−1.23
CASPT2	DZ	CAS2	no	1.94	2.02	2.14	0.37	−1.12
CASPT2	DZ	CAS3	no	1.92	2.05	2.14	0.58	−0.95
DFT	DZ		no	1.96	2.09	2.18	0.67	−0.20

SCF level. Counterions have been roughly modelized by eight charges $+1/2$ (atomic unit) placed on the faces of the triangles of the octahedron. It is the simplest way to have a neutral edifice maintaining O_h symmetry. The distance of the charges to the iron atom is of 7 Å at the equilibrium position. This distance is of the order of magnitude of the distance of the usual counterions like Li^+, Cs^+, Na^+, and K^+ found in the crystallographic data. Point charges follow the movement of the ligands in the study of the potential curves.

Fe(II) is in d^6 configuration. In O_h symmetry, the LS state is the $(t_{2g})^6$ configuration, leading to the term $^1A_{1g}$. The $(t_{2g})^5e_g$ configuration gives rise to the terms $^3T_{1g}$, $^3T_{2g}$, $^1T_{1g}$, and $^1T_{2g}$. All of them have been calculated. For the $(t_{2g})^4(e_g)^2$ configuration, only the HS state has been evaluated, namely the term $^5T_{2g}$.

3.1.2. Density Functional Theory. DFT calculations using the B3LYP functionnal[25] have been carried out using the GAUSSIAN suite of programs.[26] We have used pseudopotentials and basis sets of Dolg et al. namely, a (8s7p6d1f) contracted to [6s5p3d1f] set for iron,[27,28] a (4s4p) contracted to [2s2p] set for carbon and nitrogen, (4s) to [2s] for hydrogen. To neutralize the edifice, we have included four Na^+ atoms, lowering the symmetry to T_d. For the Na atom, the pseudopotential of Dolg was used but with a very contracted orbital ($\zeta = 10$) to avoid a spurious delocalization of the electrons on these ions.

3.2. Results. In Tables 2 and 3, we provide equilibrium distances and diabatic transition energies for the three states of interest of $Fe(CN)_6^{4-}$ and $Fe(NCH)_6^{2+}$.

3.2.1. Influence of Correlation. Table 2 gives the main results for $Fe(CN)_6^{4-}$ at the CASSCF level using CAS3 and the DZ basis set. The potential curves are very smooth with bond distances about 0.2 Å too long. Furthermore, the ordering of the states is not correct with the HS state predicted as ground state for both compounds. For an adequate description of the bonding with sufficient correlation included, one has to go beyond the CASSCF level to CASPT2.

3.2.2. Influence of Ligand Basis Sets. Calculations have been performed on $Fe(CN)_6^{4-}$ using different types of basis sets on the ligands. Results are given in Table 2. SZ basis set gives minima very different from crystallographic data (+0.2 Å error in bond length), and the difference of energy between the LS and the HS ΔE_{HL}, is of the wrong sign. This basis set clearly lacks polarization.

On the other hand, the angular polarization provided by the d orbitals in the DZP basis set does not significantly modify the results at the DZ level. In the following, we have therefore used the much cheaper DZ basis set.

3.2.3. Influence of the CAS. Results are given in Table 2 for the same $Fe(CN)_6^{4-}$ complex. The LS state is most sensitive to the choice of active space. One obtains the right bond length with CAS3 and CAS4; it confirms the necessity to include some orbitals of the ligand in the CAS for a good description of the bond. The geometries of other states are less sensitive to the choice of the CAS; it influences their energy and thus the energy gap E_{HL}. For the HS state, CAS2 and CAS4 give similar results (about 0.05 eV, the difference in ΔE_{HL} is due to different LS energies) showing that for this state, the inclusion of d correlation orbitals in the CAS is more important than the inclusion of ligand orbitals.

Although CAS4 may seem the better choice, we have performed the following calculations with CAS3 since it is cheaper and gives a quite satisfactory estimate of the metal−ligand distance. CAS4 improves the value of E_{HL} which is sensitive to many other sources of error.

3.2.4. Influence of the Point Charges. We are aware of the importance of the crystal field surrounding the molecule we deal with. An accurate treatment like the one performed by M. U. Mödl[29] is in principle possible. Here the crystal field effect is treated in a very crude manner through point charges. We have checked the sensitivity of the spectrum and potential energy curves to this description.

We have no reasonable results without point charges for the $Fe(CN)_6^{4-}$ complex. Two ways of moving the point charges away (homothetic one and constant ligand−charge distance) have been tried: the potential curves are almost identical. For the other compound, $Fe(NCH)_6^{2+}$, results are summarized in Table 3, with and without point charges. In this case, eight point charges of $-1/4$ (atomic units) have been added in the same manner as for $Fe(CN)_6^{4-}$. One does not see any qualitative influence of these point charges on the potential energy curve.

In the next section, only the $Fe(CN)_6^{4-}$ complex will be described surrounded by point charges, since they are necessary in order to obtain reasonable results. All the other complexes will be described without point charges.

3.2.5. Density Functional Theory. Calculations have been performed for both $Fe(CN)_6^{4-}$ and $Fe(NCH)_6^{2+}$ complexes. Only LS, HS, and the first triplet state have been calculated. As already mentioned, four Na^+ atoms have been added for the first compound. Results are given in Tables 2 and 3, in comparison with the CASPT2 results. All the states have a larger equilibrium distance when described by DFT than by CASPT2 (by about 0.05 Å), except for HS state of $Fe(CN)_6^{4-}$. The experimental equilibrium distances depend strongly on the crystal environment and both results are compatible with experimental information.

The value of E_{HL} does not vary with the choice of method in a systematic manner. In view of the above results, we decided to retain the CASPT2 method.

4. Comparative Study of Different Molecular Systems

4.1. Details of the Calculation. The following calculations have been performed with DZ basis set on the ligands and with CAS3. Six molecular systems have been studied: $Fe(CN)_6^{4-}$,

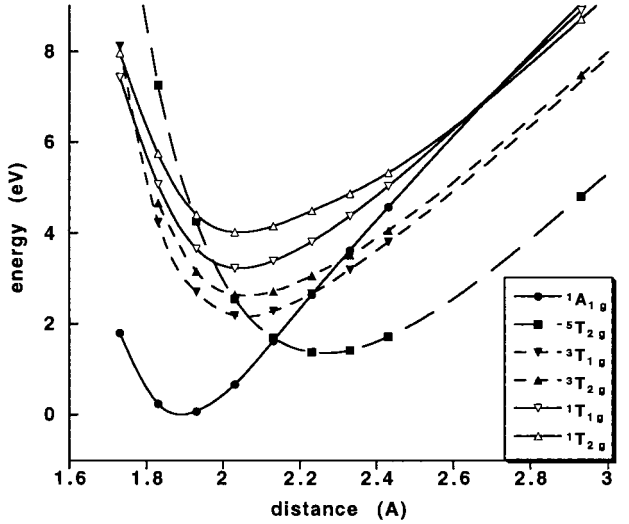

Figure 1. d → d spectrum of $Fe(CN)_6^{4-}$ as a function of Fe−C distance.

$Fe(NCH)_6^{4-}$, $Cr(CO)_6$, and $Fe(CN)_6^{3-}$ which belong to symmetry O_h, and the trans and cis isomers of $Fe(NCH)_4(CN)_2$.

The trans isomer is of D_{4h} symmetry with the two CN^- groups placed symmetrically about the iron center. The T_{1g} term is then split into $A_{2g} \oplus E_g$ and the T_{2g} term is split into $B_{2g} \oplus E_g$. The cis isomer is of C_{2v} symmetry, the CN^- ligands forming a right angle with the iron atom. In this symmetry, $A_{1g} \rightarrow A_1$, $E_g \rightarrow A_1 \oplus B_1$, $T_{1g} \rightarrow A_2 \oplus B_1 \oplus B_2$, and $T_{2g} \rightarrow A_1 \oplus A_2 \oplus B_2$.

For these two compounds, all angles have been kept as right angles, but two internal distances are now to be considered, the Fe−CN and the Fe−NCH ones. Energy minima for LS and HS states have been determined in step of 0.1 Å and potential energy curves have been calculated along a linear deformation between these two minima, keeping the internal geometries of ligands unchanged, as before.

Dissociation energies per bond have been estimated as

$$D^0 = {}^1/_6(E(\text{complex}) - 6E(\text{ligand}) - E(\text{free ion})) \quad (1)$$

The ligand energies have been determined at MP2 level and metal ion energy at CASPT2 level with CAS3, which is identical to CAS2 in this case.

4.2. Results. 4.2.1. $Fe(CN)_6^{4-}$. This compound is known as a LS compound. The experimental equilibrium distance lies between 1.90 and 1.98 Å, depending on the counterion. The C−N bond lies between 1.19 and 1.12 Å.[30] We have chosen 1.17 Å to be in agreement with previous calculations.[16] UV−visible spectra show three transitions: 2.94 eV ($^1A_{1g} \rightarrow {}^3T_{1g}$), 3.80−3.94 eV ($^1A_1 \rightarrow {}^1T_{1g}$), and 4.59−4.77 eV ($^1A_1 \rightarrow {}^1T_{2g}$) depending on the crystal structure.[31,32]

Potential curves are shown in Figure 1. They indicate the LS state as the ground state and one may note the following features: equilibrium distance, 1.89 Å; ΔR_{HL} 0.36 Å; ($^1A_{1g} \rightarrow {}^3T_{1g}$) 3.15 eV; ($^1A_{1g} \rightarrow {}^1T_{1g}$) 4.19 eV; ($^1A_{1g} \rightarrow {}^1T_{2g}$) 4.87 eV; and dissociation energy: 6.19 eV per bond.

The triplet state is never the ground state, at all metal−ligand distances. The equilibrium distance is reasonable, and vertical transitions are overestimated by 0.2 eV only.

4.2.2. $Fe(NCH)_6^{2+}$. This compound is a HS complex. Crystallographic data give a metal−ligand distance of 2.16 Å and a N−C distance of 1.10 Å. Calculations have been performed using this latter value. UV−visible spectrum shows a band at 1.48 eV which corresponds to the $^5T_{2g} \rightarrow {}^5E_g$ transition.[33−35]

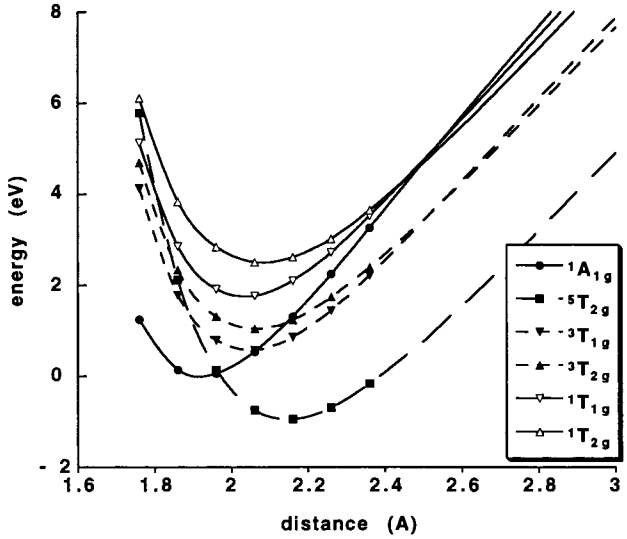

Figure 2. d → d spectrum of $Fe(NCH)_6^{2+}$ as a function of Fe−N distance.

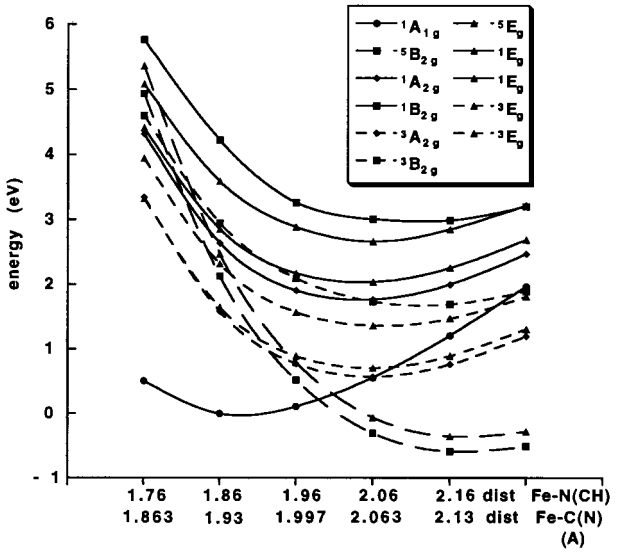

Figure 3. d → d spectrum of the trans isomer of $Fe(NCH)_4(CN)_2$ as a function of Fe−ligand distance.

Curves shown in Figure 2 indicate that the ground state multiplicity is correct, with the following characteristics: equilibrium distance 2.14 Å; ΔR_{HL} 0.22 Å; vertical transition $^5T_{2g} \rightarrow {}^5E_g$ 1.46 eV; and dissociation energy 3.24 eV per bond.

Again, the triplet state is never found to be the ground state. Equilibrium distance and the vertical transition are correct. The dissociation energy is half of the previous one: it is expected to be smaller from electrostatic arguments: since the ligands are neutral, there is no charge−charge attraction term.

4.2.3. *cis*- and *trans*-$Fe(CN)_2(NCH)_4$. To our knowledge, no information is available about these compounds. Structures of Fe(II) and Ru(II) complexes with two cyanato and N-bonding ligands have been found, some of them being trans, some of them being cis.

The curves of Figure 3 and 4 support the following conclusions:

1. All states of the trans isomer are more stable than the corresponding cis isomer states. Both of them have the HS state for ground state. The gap of energy E_{HL} is greater for the trans isomer and has the mean value of the "pure" compounds weighted by the number of ligands ($E_{HL}^{trans} = {}^2/_3 E_{HL}^{NCH} + {}^1/_3 E_{HL}^{CN}$).

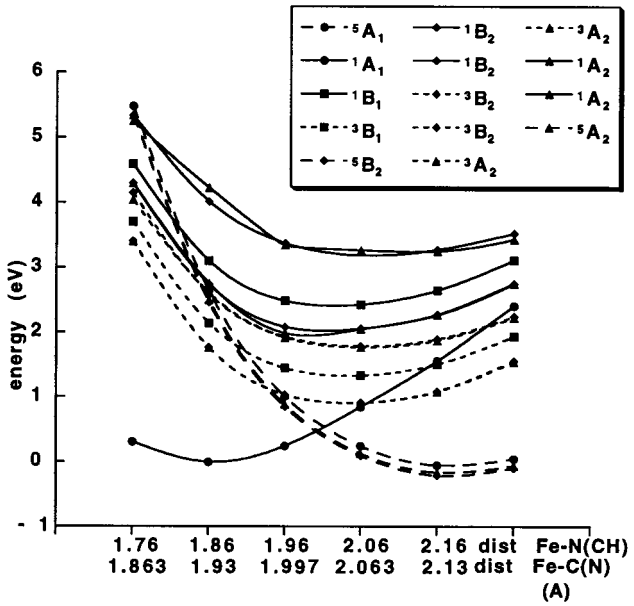

Figure 4. d → d spectrum of the cis isomer of $Fe(NCH)_4(CN)_2$ as a function of Fe−ligand distance.

2. Equilibrium distances are the same for both compounds: for LS state, r(Fe−NCH) = 1.88 Å, r(Fe−CN) = 1.95 Å; for HS state, r(Fe−NCH) = 2.17 Å, r(Fe−CN) = 2.14 Å.

The Fe−CN distance of the LS state is slightly larger than in $Fe(CN)_6^{4-}$, and the Fe−NCH distance of HS state is more or less the same as in $Fe(NCH)_6^{2+}$.

3. The largest splitting of the energy states due to the lowering of the symmetry is of 0.4 eV in the HS of the cis compound. The other states are split by about 0.2 eV.

For none of these compounds does the triplet state become the ground state for intermediate distances.

4.2.4. $Cr(CO)_6$. This compound is a LS one. The experimental Cr−C distance is 1.914 Å and the C−O distance 1.14 Å. UV−visible spectrum is not completely understood: d → d absorption bands are in the same energy range as the metal−ligands charge transfer bands.[36] Two bands are observed, one at 4.43 eV and one at 5.41 eV, their assignments being a matter of controversy. The precise calculation of this spectrum has been the object of many calculations.[37−40] Many experiments have been done to determine the values of bond dissociation of complexes $Cr(CO)_x^+$ in the gas phase:[41,42] for $x = 6$, it equals 0.93 eV, and for $x = 5$, it equals 1.35 eV. Although these compounds are charged, it gives an estimate of the magnitude of this energy: the dissociation energy of $Cr(CO)_6$ should be smaller than the corresponding value above due to the absence of polarization forces.

The curves of Figure 5 give the following values: equilibrium distance 1.89 Å; ΔR_{HL} 0.30 Å; ($^1A_{1g} \rightarrow {}^3T_{1g}$) 4.68 eV; ($^1A_{1g} \rightarrow {}^3T_{2g}$) 5.03 eV; ($^1A_{1g} \rightarrow {}^1T_{1g}$) 5.12 eV; ($^1A_{1g} \rightarrow {}^1T_{2g}$) 5.22 eV; and dissociation energy 1.05 eV per bond.

The LS state is clearly the ground state. In its lowest energy geometry, the HS state is above the LS one: this state should have a much shorter lifetime than when it appears as a secondary minimum in the overall (post spin−orbit) lowest potential energy surface, as occurred in $Fe(CN)_6^{4-}$. The equilibrium distance is in accuracy with crystallographic data. Vertical transitions are in the right region whereas the dissociation energy seems to be slightly too large.

4.2.5. $Fe(CN)_6^{3-}$. This compound is a LS one. Numerous crystallographic data exist for this ion ranging from 1.908 to 1.968 Å for the Fe−C bond and 1.23 to 2.23 Å for the C−N bond.[43,44] In most cases, however, the second distance lies in the range of 1.14−1.15 Å. We have performed our calculations using a distance C−N of 1.15 Å. The UV−visible spectrum depends strongly on experimental conditions. In ref 31, ($^2T_{2g} \rightarrow {}^2T_{1g}$) and ($^2T_{2g} \rightarrow {}^2A_{2g}$) appear at 3.87 eV and ($^2T_{2g} \rightarrow {}^2E_g$) at 4.43 eV. In ref 45, these bands appears at 3.69, 3.74, and 4.12 eV, respectively, ($^2T_{2g} \rightarrow {}^4T_{1g}$) at 2.23 eV, and ($^2T_{2g} \rightarrow {}^6A_{1g}$) at 3.34 eV.

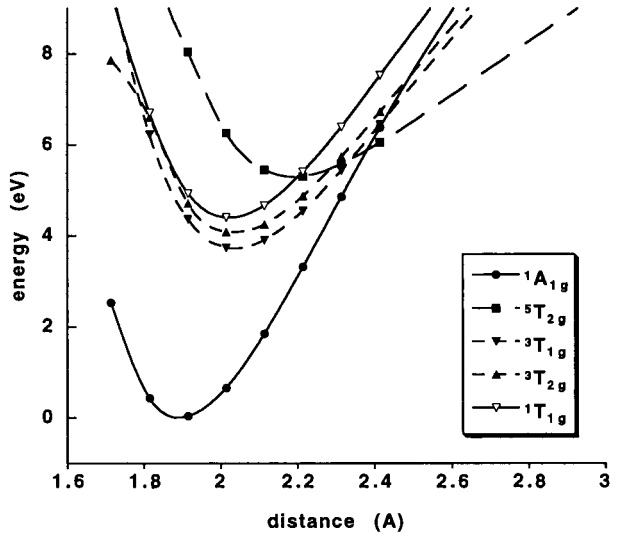

Figure 5. d → d spectrum of $Cr(CO)_6$ as a function of Cr−C distance.

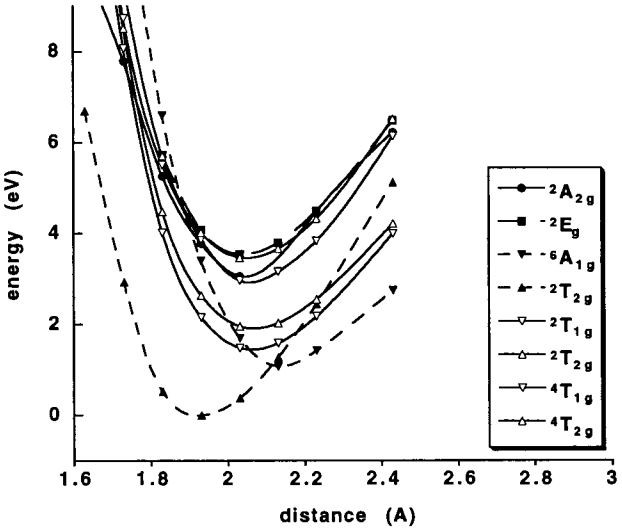

Figure 6. d → d spectrum of $Fe(CN)_6^{3-}$ as a function of Fe−C distance.

The curves of Figure 6 give the LS state as ground state and the following characteristics: equilibrium distance: 1.92 Å; ΔR_{HL} 0.22 Å; ($^2T_{2g} \rightarrow {}^4T_{2g}$) 2.27 eV; ($^2T_{2g} \rightarrow {}^2T_{1g}$) 4.01 eV; ($^2T_{2g} \rightarrow {}^2A_{2g}$) 3.89 eV; ($^2T_{2g} \rightarrow {}^2E_g$) 4.20 eV; ($^2T_{2g} \rightarrow {}^6A_{1g}$) 3.63 eV; and dissociation energy: 10.5 eV per bond.

For this molecule, the results are in accordance with the available experimental data.

5. Crystal Field Parameters

Racah's parameters B and C and the ligand field parameter Δ can be extracted from these ab initio spectra in the same manner as from an experimental UV−visible spectrum. We have done so and will discuss the distance dependence of these parameters.

5.1. Racah's Parameters *B* and *C* and Crystal Field Parameter Δ. 5.1.1. Extraction of the Parameters. Based on symmetry arguments, it can be shown that the first-order electrostatic energies of the states of the free ion can be expressed in terms of three parameters *A*, *B*, and *C*, Racah's parameters. They characterize the repulsion of the electrons on the metal center. The *A* parameter does not enter in the energy differences between states with the same d^n configuration.[46] For free Fe(II), $B = 939$ cm^{-1} and $C = 3720$ cm^{-1}.[24] For free Cr(0), $B = 790$ cm^{-1} and $C = 2520$ cm^{-1}.

To a first approximation, the complex ion can be seen as a metal ion placed in the electrostatic field of the ligands, without any further interaction. In such a case, in O_h symmetry, the energies of the d orbitals are split into two groups, t_{2g} and e_g, separated by an energy Δ. The electron−electron repulsion terms are identical to those of the free ion, with lowered values of *B* and *C* because of the slight delocalization of the d orbitals on the ligands. The monoelectronic part is expressed in terms of Δ, depending on the number of electrons occupying the e_g orbitals: if the monoelectronic reference is the LS state, exciting one electron to the e_g orbitals costs Δ, two electrons 2Δ.

Under such conditions, for each irreducible representation Γ, matrix elements of the Hamiltonian for a d^n configuration take the following form:

$$\langle t_{2g}^{n-l}\, e_g^{l} | H | t_{2g}^{n-l'}\, e_g^{l'} \rangle = f^{\Gamma}_{nll'}(A, B, C) + \delta_{ll'} l\Delta \qquad (2)$$

where $\delta_{ll'}$ is the Kronecker symbol and $f^{\Gamma}_{nll'}(A, B, C)$ is a function of *A*, *B*, and *C*.

Diagonalizing the corresponding matrices gives an expression of the lowest roots in terms of *A*, *B*, *C*, and Δ. As already pointed out, differences of energies of the d → d spectrum do not depend on the value of *A*.

For the compounds considered, five or six transition energies have been evaluated at several geometries; parameters Δ, *B*, and *C* can be extracted for each distance by a mean square fit. Usually, the extraction of these parameters from UV−visible spectra neglects nondiagonal terms ($l \neq l'$); this assumption is valid for large values of Δ, as diagonal terms then are large compared to the nondiagonal ones. In such a description, each state is described by only one configuration. Δ tends to zero at large distances and the spectrum becomes that of the free ion.

The $Fe(CN)_2(NCH)_4$ molecule does not have O_h symmetry; terms degenerate in octahedral symmetry are no longer degenerate. However, our results presented in section 4.2.3 show that this splitting is a small perturbation and that the main features of the curves are the same as in O_h symmetry. Energies of octahedral terms have therefore been replaced by the mean value of the different states issued from this term, and the metal−ligand distance has been chosen as the weighted mean of the metal−ligand distances in the molecule.

All extractions are based on the minimization of the mean deviation:

$$\mathrm{err} = \left[\frac{1}{N}\sum_{i=1}^{N}(f_i(\Delta,B,C) - E_i)^2\right]^{1/2} \qquad (3)$$

where f_i is the analytical expression of the *i*th transition and E_i is its calculated value, the extraction being performed with *N* transitions.

5.1.2. Ligand Field Theory and Crystal Field Theory. There are two models for the origin of the crystal field: the *crystal field theory* based on electrostatic arguments and the *ligand field theory* based on the theory of molecular orbitals.

In crystal field theory, ligands are modelized by charges or dipoles, and e_g orbitals are destabilized because they point toward them. The crystal field parameter can be expressed in the following way:[46]

$$\Delta = 5\gamma\overline{r^4} \qquad (4)$$

where γ characterizes the electrostatic environment and $\overline{r^4}$ is the mean value of r^4 for the considered d orbital, which is assumed to have the same radial extension in t_{2g} and e_g symmetries. When ligands are modelized by six charges *Q* at a distance *R* from the metal ion, the γ parameter is given by

$$\gamma = -Q/12\pi\epsilon_0 R^5 \qquad (5)$$

When the ligands are modelized by six point dipoles of strength *d* pointing toward the origin at distance *R* from the origin

$$\gamma = -4d/12\pi\epsilon_0 R^6 \qquad (6)$$

Equation 4 can be easily generalized to the cis and trans compounds; one obtains the same expression for both cases:

$$\Delta = 5\frac{\gamma^{(1)} + 2\,\gamma^{(2)}}{3}\overline{r^4} \qquad (7)$$

where $\gamma^{(i)}$ characterizes the two different environments, assuming there are two ligands of type (1) and four of type (2). It is simply the weighted mean value of the ligand field for a compound with only ligands (1) and of the ligand field of the compound with only ligands (2).

In the 1950s, ligand field theory was proposed as an alternative explanatory model. Based on molecular orbital theory, it is able to explain most of the experimental features. Ligands with extended and high-energy σ nonbonding orbitals directed toward the metal will interact strongly with the $d^*_{e_g}$ orbitals, enhancing the splitting between these orbitals and the quasi nonbonding $d_{t_{2g}}$ orbitals. Thus, the ligand field increases with larger σ-donor effect of the ligand.

π-donor ligands have high-energy π orbitals. In O_h symmetry, they combine with the metal $d_{t_{2g}}$ orbitals, which then becomes slightly antibonding. This tends to reduce Δ. On the other hand, π-acceptor ligands have low-energy π^* orbitals which, combined with $d_{t_{2g}}$, makes the latter slightly bonding. This tends to enhance Δ.[47]

The variation of the ligand field parameter in such a model is expected to decrease exponentially with metal−ligand distance, as do the overlaps between metal and ligands orbitals.

5.2. Results and Discussion. Table 4 sums up some characteristics of the fits. The extraction results in a quite small mean deviation, always smaller than 1000 cm^{-1} and even smaller about 100 cm^{-1} for some compounds, compared to transitions energies always greater than 10 000 cm^{-1}. The corresponding deviation is 931 cm^{-1} for the free Fe(II).

Variations of *B* and *C* are plotted in Figure 7. Their values for LS and HS geometries are given in Table 4. As expected, their variation is not too large; *B* stays at about half its value in free ion while *C* increases slightly with distance. For comparison, values of *B* and *C* extracted from the experimental spectrum of $Fe(CN)_6^{4-}$ with the three known transitions is $B = 378$ cm^{-1} and $C = 3629$ cm^{-1}. Within the one-configuration approximation, the extraction from the calculated spectrum gives $B = 392$

TABLE 4: Extraction of Racah's Parameters and of the Crystal Field Parameter[a]

	B_{LS}, cm^{-1}	B_{HS}, cm^{-1}	C_{LS}, cm^{-1}	C_{HS}, cm^{-1}	Δ^b A, eV	Δ^b β, Å^{-2}	err_{LS}, cm^{-1}	err_{HS}, cm^{-1}
$Cr(CO)_6$	244	307	1659	2488	45.7	0.60	439	964
$Fe(CN)_6^{3-}$	342	328	3838	4467	44.4	0.63	485	1026
$Fe(CN)_6^{4-}$	438	580	3522	4305	55.9	0.72	148	188
$Fe(NCH)_6^{2+}$	698	539	4181	4740	78.6	0.93	105	221
trans-$Fe(NCH)_4(CN)_2$	779	844	3338	4166	40.8	0.74	856	912
cis-$Fe(NCH)_4(CN)_2$	690	790	3246	3889	67.1	0.88	371	1149

[a] B and C and the mean deviation are given for the LS and HS equilibrium geometries, Δ is characterized by an exponential law. [b] $\Delta = Ae^{-\beta R^2}$.

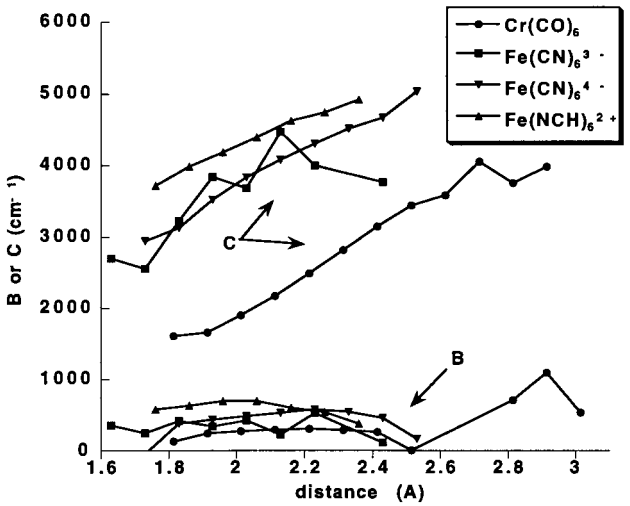

Figure 7. Racah's parameters B and C as functions of metal−ligand distance for the different compounds.

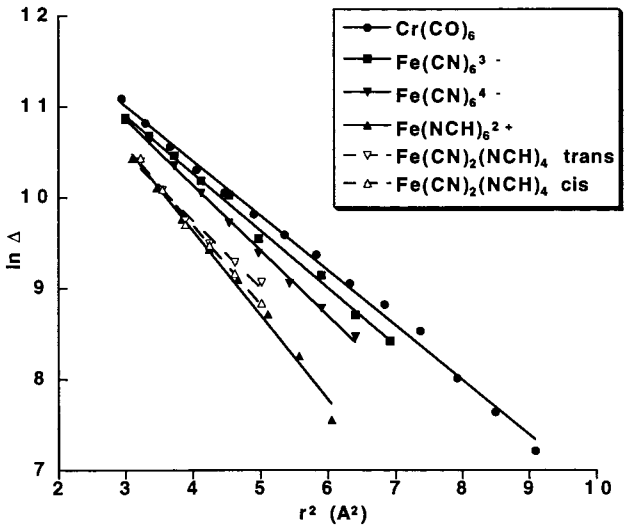

Figure 8. Variation of Δ as a function of metal−ligand distance for the different compounds. Δ is expressed in cm^{-1}.

cm^{-1} and $C = 3633$ cm^{-1}, and with the full matrices $B = 438$ cm^{-1} and $C = 3522$ cm^{-1}.

Variations of Δ are plotted in Figure 8. This is a ln(Δ) vs R^2 plot. One obtains almost straight lines; the behavior is well described by an exponentional law:

$$\Delta = Ae^{-\beta R^2} \tag{8}$$

where R is the distance between the metal ion and the bonding atom. In the terms of ligand field theory, the variation of the ligand field parameter is determined by the overlap between metal and ligand orbitals, which should vary as $e^{-\beta R}$. In our modelization, orbitals are described by the mean of Gaussian functions, whose overlaps vary as $e^{-\beta R^2}$. The variation obtained in eq 8 is in accordance with ligand field theory.

All the characteristics of these plots are summarized in Table 4. The one-configuration approximation is reasonable for short distances till around 2 Å, but fails completely for large distances as Δ diminishes. Figure 8 is compatible with spectrochemical series; ligand or metal ions are classified in order of increasing Δ_0, the value of Δ at equilibrium: NCH < CN^-, Fe^{2+} < Fe^{3+}. From our results, the greater the strength of the ligand field, the smaller are both A and β. It shows that a strong-field compound has a stronger crystal field than a low-field compound, whatever the metal−ligand distance. At short distances, between 1.5 and 3. Å, the behavior is well described by a power law:

$$\Delta = \alpha/R^n \tag{9}$$

with exponents lying between 5 and 6 in agreement with crystal field theory. For larger distances, the slope of the ln Δ vs ln R plot increases, meaning the formal exponent n increases. It shows that the crystal field theory predicts the suitable behavior in the range of the equilibrium distances, but that a power law is not suitable with a pure electrostatic model at large distances. It is quite surprising that such a model gives the right exponent in the range where delocalization is the greater and seemingly independent of the bonding: $Cr(CO)_6$ is predominated by the high π-back bonding, while in $Fe(CN)_6^{4-}$ all the fragments are charged.

The only experimental work to our knowledge is a study of the pressure dependence of Δ in NiO by Drickamer.[48] He found a R^{-5} dependence but in a small region of distances. It has later been shown that it can be reproduced by an exponential law as well.[49]

5.3. Energy Gap between LS and HS States. In the region of interest, namely in the range of the equilibrium distances of the LS and HS states, the ligand field parameter is equally well described by an exponential law and a power law with exponent in the range of 5−6. We seek a description of the spectra with as few parameters as possible. In such a small range of distance, a single parameter is enough to reproduce very well the data. Let us assume $\Delta = \alpha R^{-6}$. α equals 203, 197, 182, and 128 eV Å^{-6} for $Cr(CO)_6$, $Fe(CN)_6^{3-}$, $Fe(CN)_6^{4-}$, and $Fe(NCH)_6^{2+}$, respectively. With such a law, values of the prefactor α follow the spectrochemical series.

To roughly modelize the effect of ligand field strength on the spin-transition phenomenon, the curve of LS state is taken from the $Fe(CN)_6^{4-}$ complex. The HS state is deduced from this curve using the values of B, C, and Δ. The set of curves of Figure 9 are plotted with B and C kept constant and the ligand field parameter given by

$$\Delta = y\alpha/R^6 \tag{10}$$

where α is fixed. In the frame of this simple model, increasing

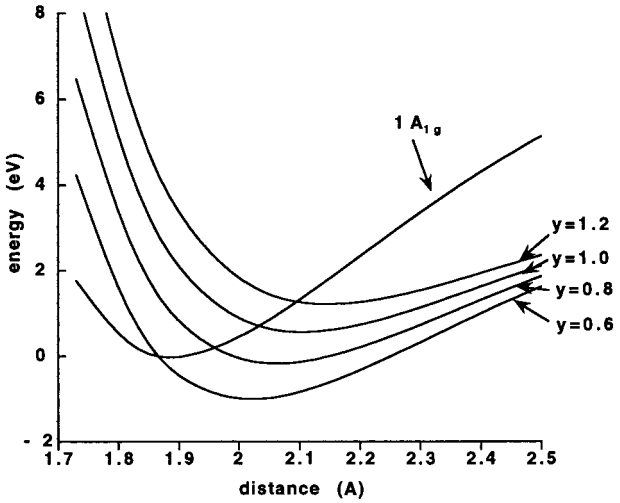

Figure 9. Model curves for LS and HS states. LS state is the one for $Fe(CN)_6^{4-}$. HS curve is deduced from the former one with $B = 0.05$ eV, $C = 0.5$ eV and $\Delta = y \times 150/R^6$ eV, R in Å, for different values of y.

parameter y permits the transformation of a LS compound into a HS one. The value of the energy gap E_{HL} varies almost linearly with y, and the difference Δr_{HL} of equilibrium distances between the two states tends to decrease with the strength of the crystal field.

6. Conclusion

Ab initio calculations have been performed for several d^6 octahedral coordination compounds: $Cr(CO)_6$, chosen for its high-covalent character and its strong π back-donation, two octahedral complexes of iron(II), the low-spin $Fe(CN)_6^{4-}$, and the high-spin $Fe(NCH)_6^{2+}$; two mixed complexes whose geometries are not strictly octahedral $Fe(NCH)_4(CN)_2$, in the trans and cis conformations; and finally, a d^5 compound, $Fe(CN)_6^{3-}$.

All these compounds have been studied in terms of the metal−ligand distance. The proposed calculations are in agreement with the main experimental data. The CASPT2 ab initio calculations give the preferred ground state multiplicity (ie the signe of E_{HL}), namely HS for $Fe(NCH)_6^{2+}$ and LS for $Fe(CN)_6^{4-}$ and $Fe(CN)_6^{3-}$. The calculated metal−ligand distances are in very good agreement with crystallographic data, and the vertical spectra agree with the experimental transition energies within 0.2 eV. The dissociation energies seem to be reasonable. The differences of equilibrium distances between LS and HS states Δr_{HL} lie in the 0.2−0.3 Å range. This parameter is only known for complexes exhibiting a spin transition: for instance, in the case of the $Fe(bpy)_2(NCS)_2$, where bpy = 2,2′-bipyridine, $\Delta r_{HL} = 0.1$ Å for the thiocyanato group and $\Delta r_{HL} = 0.21$ Å for the bipyridine.[12] This distance seems to increase with the strength of ligand field (see sections 4.2 and 5.3).

The study of the two mixed complexes has revealed valuable information: the main features of an octahedral environment is recovered, and the splitting of the states due to the lowering of the symmetry is small, about 0.2 eV. The equilibrium distance between the metal and a ligand is the same as in the complex with only this type of ligands, in both LS and HS states; the equilibrium distances are slightly perturbed by the nature of the ligands of the other bonds. Ligand field parameter for both compounds and the energy gap between LS and HS states for the trans compounds are the mean values of the compounds with only one type of ligands weighted by the number of the ligands.

An important information, which is not easily obtained from experiment concerns the position and the shape of the triplet state potential curves. They systematically present a minimum close to the intermediate $R^{\#}$ distance where the HS and LS potential curves cross. Estimated from the cis compound for which $E_{HL} \approx 0$, the minimum of the lowest triplet state is about 0.5 eV above the crossing point and the activation barrier between LS and HS wells is of the same order of magnitude. Since HS and LS states differ by two orbitals, they do not interact at first order through the monoelectronic spin−orbit operator. Our potential curves may be used to propose a rough evaluation of the second-order effective coupling between HS and LS:

$$H^{\text{eff}}_{\text{HS,LS}} = \frac{\langle \text{HS}|H|\text{TS}\rangle\langle \text{TS}|H|\text{LS}\rangle}{E_{\text{LS}} - E_{\text{TS}}} \qquad (11)$$

where TS represents the triplet state, E_{LS} and E_{TS} are the energies of the LS and TS states at $R^{\#}$, and $\langle \text{HS}|H|\text{TS}\rangle$ is the coupling via the full Hamiltonian between HS and TS states: it has been evaluated at 400 cm^{-1}, the order of magnitude of spin−orbit coupling constant in the free ion. Within this frame, we can estimate that (i) $H^{\text{eff}}_{\text{HS,LS}}$ should be small ($\approx$40 cm^{-1}) at the crossing geometry, while the barrier height is about 4000 cm^{-1} and (ii) $H^{\text{eff}}_{\text{HS,LS}}$ should decrease rapidly when moving away from this crossing point, due the evolution of the energy denominator in eq 11.

Finally, Racah's parameters and the ligand field parameter have been extracted from the calculated potential curves which permits to study their dependancy of metal−ligand distance. B is almost constant at about half its value in the free ions and C increases slightly with distance. Δ is very well described by an exponential law compatible with ligand field theory. In the range of the equilibrium distances, the one-configuration approximation appears valid and a power law is as good as the previous one able to reproduce the data; in such a frame, the exponents obtained are compatible with crystal field theory.

Acknowledgment. The Laboratoire de Physique Quantique is Unité Mixte de Recherches du CNRS: UMR 5626. This work has been supported by a TMR contract of the European Commission (QUCEX FMRX-CT 960079). The author thanks Jean-Paul Malrieu and Trond Saue for their help and for their interest in this work.

References and Notes

(1) Kahn, O. *Molecular Magnetism*; VCH: New York, 1993.
(2) Gütlich; P.; Hauser, A.; Spiering; H. *Angew. Chem., Int. Ed. Engl.* **1994**, *33*, 2024.
(3) König, E. *Struct. Bonding (Berlin)* **1991**, *76*, 51.
(4) Gütlich, P.; Hauser, A. *Coord. Chem. Rev.* **1990**, *97*, 1.
(5) Wajnflasz, J. *Phys. Stat. Solidi* **1970**, *40*, 537.
(6) Bari, R. A.; Sivardière, J. J. *Phys. Rev. B* **1972**, *5*, 4466.
(7) Bousseksou, A.; Nasser, J.; Linares, J.; Boukheddaden, K.; Varret, F. *J. Phys. I Fr.* **1992**, *2*, 1381.
(8) Bolvin, H.; Kahn, O. *Chem. Phys.* **1995**, *192*, 295.
(9) Descurtins, S.; Gütlich, P.; Köhler, C. P.; Spiering, H.; Hauser, A. *Chem. Phys. Lett.* **1984**, *139*, 1.
(10) Descurtins, S.; Gütlich, P.; Hasselbach, K. M.; Spiering, H.; Hauser, A. *Inorg. Chem.* **1985**, *24*, 2174.
(11) Jeftić, J.; Hauser, A. *Chem. Phys. Lett.* **1996**, *248*, 458.
(12) Konno, M.; Mimami-Kido, M. *Bull. Chem. Soc. Jpn.* **1991**, *64*, 339.
(13) Roos, B. O.; Andersson, K.; Fülscher, M. P.; Malmqvist, P.-A.; Serrano-Andrès, L.; Pierloot, K.; Merchàn, M. *In Advances in Chemical Physics: New methods in Computational Quantum Mechanics;* Prigogine, I., Rice, S. A., Eds.; John Wiley & Sons: New York, 1996; Vol. XCIII, p 219.

(14) Andersson, K.; Roos, B. O. In *Modern electron structure theory;* Yarkony, R., Ed.; Advanced Series in Physical Chemistry; Wolrd Scientific Publishing Co. Pte. Ltd.: Singapore, 1995; Vol. 2, Part I, p 55.

(15) Pierloot, K.; De Kerpel, J. O. A.; Ryde, U.; Roos, B. O. *J. Am. Chem. Soc.* **1997**, *119*, 218.

(16) Pierloot, K.; Van Praet, E.; Vanquickenborne, L. G. *J. Phys. Chem.* **1993**, *97*, 1220.

(17) Pierloot, K.; Dumez, B.; Widmark, P.-O.; Roos, B. O. *Theor. Chim. Acta* **1995**, *90*, 87.

(18) Andersson, K.; Malmqvist, P.-Å.; Roos, B. O.; Sadlej, A. J.; Wolinski, K. *J. Phys. Chem.* **1990**, *94*, 5483.

(19) Andersson, K.; Fülscher, M. P.; Karlström, G.; Lindh, R.; Malmqvist, P.-Å.; Olsen, J.; Roos, B. O.; Sadlej, A. J.; Blomberg, M. R. A.; Siegbahn, P. E. M.; Kelló, V.; Noga, J.; Urban, M.; Widmark, P.-O. MOLCAS Version 3; Dept. of Theor. Chem., Chem. Center, University of Lund, P.O.B. 124, S-221 00 Lund, Sweden, 1994.

(20) Ben Amor, N.; Maynau, D. CASDI, Toulouse, 1997.

(21) Malmqvist, P.-Å.; Rendell, A.; Roos, B. O. *J. Phys. Chem.* **1990**, *94*, 5477.

(22) Miralles, J.; Castell, O.; Caballol, R.; Malrieu, J. P. *Chem. Phys.* **1993,** *172*, 33.

(23) Moore, C. E. *Atomic Energy Levels*; Natl. Bur. Stand. (U.S.) Circ. No. 467; U.S. GPO: Washington, D.C., 1949.

(24) Trees, R. E. *Phys. Rev.* **1951**, *82*, 683.

(25) Lee, C.; Yang, W.; Parr, R. G. *Phys. Rev.* B **1988**, *37*, 785.

(26) *Gaussian 94*, Revision B.4; Frisch, M. J.; Trucks, G. W.; Schlegel, H. B.; Gill, BP. M. W.; Johnson, B. G.; Robb, M. A.; Cheeseman, J. R.; Keith, T.; Petersson, G. A.; Montgomery, A.; Raghavachari, K.; Al-Laham, M. A.; Zakrzewski, V. G.; Ortiz, J. V.; Foresman, J. B.; Peng, C. Y.; Ayala, P. Y.; Chen, W.; Wong, M. W.; Andres, J. L.; Replogle, E. S.; Gomperts, R.; Martin, R. L.; Fox, D. J.; Binkley, J. S.; Defrees, D. J.; Baker, J.; Steward, J. P.; Head-Gordon, M.; Gonzalez, C.; Pople, J. A. GAUSSIAN, Inc., Pitsburgh PA, 1995.

(27) Bergner, A.; Dolg, M.; Kuechle, W.; Stoll, H.; Preuss, H. *Mol. Phys.* **1993**, *80*, 1431.

(28) Dolg, M.; Wedig, U.; Stoll, H.; Preuss, H. *J. Chem. Phys.* **1987**, *86*, 866.

(29) Mödl, M. U. Doktorarbeit, Dresden, 1995.

(30) Meyer, H. J.; Pickardt, J. *Acta Crystallogr., Sect. C* **1988**, *44*, 1715.

(31) Alexander, J. J.; Gray, H. B. *J. Am. Chem. Soc.* **1968**, *90*, 4260.

(32) Ayers, J. B.; Wagoner, W. H. *Inorg. Nucl. Chem. (Munich)* **1974**, *92*, 721.

(33) Constant, G.; Daran, J. C.; Jeannin, Y. C. *R. Acad. Sci. Paris* **1967**, *265*, 808.

(34) Constant, G.; Daran, J. C.; Jeannin, Y. *J. Solid State Chem.* **1970**, *2*, 421.

(35) Constant, G.; Daran, J. C.; Jeannin, Y. *J. Inorg. Nucl. Chem.* **1973**, *55*, 493.

(36) Beach, N. A.; Gray, H. B. *J. Am. Chem. Soc.* **1968**, *90*, 5713.

(37) Kotzian, M.; Rösch, N.; Schóder, H.; Zerner, M. C. *J. Am. Chem. Soc.* **1989**, *111*, 7687.

(38) Pierloot, K.; Tsokos, E.; Vanquickenborne, L. G. *J. Phys. Chem.* **1996**, *100*, 16545.

(39) Daniel, C.; Veillard, A.; Strich, A. Private communication.

(40) Pollak, C.; Rosa, E.; Baerends, E. J. *J. Am. Chem. Soc.* **1997**, *119*, 7324.

(41) Schultz, R. H.; Crellin, K. C.; Armentrout, P. B. *J. Am. Chem. Soc.* **1991**, *113*, 8590.

(42) Khan, F. A.; Clemmer, D. E.; Schultz, R. H.; Armentrout, P. B. *J. Phys. Chem.* **1993**, *97*, 7978.

(43) Bok, L. D. C.; Leipoldt, J. G.; Basson, S. S. *Z. Anorg. Allg. Chem.* **1972**, *389*, 307.

(44) Pickardt, J.; Kahler, J.; Rautenberg, N.; Riedel, E. *Z. Naturforsch., Teil B* **1984**, *39*, 1162.

(45) Gale, B.; McCaffery, A. J. *J. Chem. Soc., Dalton Trans* **1973**, 1344.

(46) Griffith, J. S. *The theory of transition-metal ions;* Cambridge University Press: Cambridge, UK, 1964.

(47) Purcell, K. F.; Kotz, J. C. *Inorganic Chemistry*; Holt-Saunders International Editions: Philadelphia, PA, 1977.

(48) Drickamer, H. G. *J. Chem. Phys.* **1967**, *47*, 1880.

(49) Smith, D. W. *J. Chem. Phys.* **1969**, *50*, 2784.